



## Empirical modelling and statistical analysis of axial load capacity in square hollow concrete columns

Damini Righteous Gilbert<sup>1</sup>, Timothy Omotoyosi Awanu<sup>2</sup>

<sup>1</sup> Department of Civil Engineering, Federal University, Otuoke, Bayelsa State, Nigeria

<sup>2</sup> School of Engineering, Institute of Entrepreneurship and Vocational Training, Bayelsa State, Nigeria

### Abstract

This paper presents an empirical and statistical study on the axial load capacity of square hollow concrete columns (SHCCs) with central voids, with and without reinforcement, subjected to short-term (28 days) and mid-term (56 days) curing. An experimental program investigated 72 SHCCs of varying slenderness ratios ( $L/D = 1$  to 10) and concrete mix designs. Axial compression tests were performed to evaluate the ultimate load capacity ( $P_u$ ). Results demonstrated that increased slenderness significantly reduces capacity, with a 75% reduction observed (from 456.6 kN to 116.12 kN) for reinforced high-strength (RC-25) columns as  $L/D$  increased from 1 to 10 at 28 days. Concrete mix grade was a dominant factor, with a 38% increase in  $P_u$  (from 153.75 kN to 212.09 kN) for the RC-25 mix compared to RC-15 at a constant  $L/D$  ratio of 5. Curing age significantly improved axial strength, with mid-term specimens exhibiting strength gains of up to 23.8% (from 308.0 kN to 381.25 kN for RC-25 at  $L/D=3$ ). Furthermore, steel reinforcement substantially increased capacity, with reinforced specimens achieving over 100% higher loads than plain concrete sections of equivalent geometry. Statistical analysis via ANOVA confirmed the high significance of these factors ( $F$ -value = 2212.60,  $p < 0.0001$ ), and linear regression yielded highly reliable empirical predictive models (Adjusted  $R^2 = 0.9894$ ). The findings demonstrate that empirical-statistical modeling, informed by key parameters of slenderness, material strength, and curing, provides a robust and practical tool for optimizing the design of SHCCs.

**Keywords:** Square hollow concrete columns, axial load capacity, empirical modeling, slenderness ratio, regression

### Introduction

The use of hollow reinforced concrete columns has become increasingly prominent in contemporary construction due to their ability to reduce self-weight while maintaining structural efficiency. These columns offer improved material economy and functional adaptability, particularly in high-rise buildings, bridge piers, and service infrastructure, where reduced dead load and internal space for utilities are advantageous (Zhao *et al.*, 2021; Ali *et al.*, 2023) [3, 39]. Compared with solid columns, hollow sections not only reduce the demand on foundations but also contribute to enhanced sustainability by lowering material consumption. Among hollow geometries, square hollow columns represent a distinct category with unique mechanical characteristics. Their planar geometry facilitates easier reinforcement placement and formwork, while their torsional stiffness and axial load resistance render them effective alternatives to circular hollow columns in certain applications (Hadi and Youssf, 2020; Abbas *et al.*, 2022) [1, 22]. Previous investigations have highlighted that parameters such as hollow-core ratio, wall thickness, reinforcement configuration, and curing conditions substantially affect the axial load behaviour and failure modes of these columns (Yang *et al.*, 2021; Mohammed *et al.*, 2024) [28, 38]. Despite these insights, most available studies focus on specialized configurations, such as concrete-filled steel tubes (CFST), fibre-reinforced polymer (FRP)-confined hollow columns, or high-strength concretes, with limited emphasis on plain reinforced square hollow concrete columns.

The lack of systematic, statistically validated empirical models for square hollow reinforced columns represents a critical gap in structural design research. Reliable predictive models are necessary for practical applications such as

preliminary sizing, safety assessments, and code development. Current design provisions are largely calibrated against data from solid or circular columns, which do not always capture the nuanced performance of hollow geometries (Fawzy and Nasr, 2022) [20]. Moreover, curing age effects, though well documented in general concrete behaviour, are not consistently integrated into predictive models for hollow column configurations.

In recent years, data-driven modelling techniques, including regression analysis, artificial neural networks, and ensemble learning, have emerged as powerful tools for predicting structural behaviour under axial loads (Awoyera *et al.*, 2021; Chou and Pham, 2023) [7, 17]. While machine learning (ML) approaches can capture complex nonlinearities, their lack of transparency often limits their direct applicability in engineering design practice. By contrast, regression-based models, when rigorously validated through statistical methods such as analysis of variance (ANOVA), provide interpretable and reliable predictive tools. Best practice therefore advocates a hybrid approach: experimental validation, empirical regression modelling, and statistical verification, supplemented by data-driven methods where appropriate (Li *et al.*, 2022) [24].

Against this backdrop, the present study investigates the axial load behaviour of square hollow reinforced concrete columns subjected to compression testing at 28 and 56 days. The experimental program evaluated variations in mix proportions, slenderness ratios, and curing periods, generating a dataset suitable for empirical modelling. Regression equations were subsequently developed to predict axial load capacity explicitly incorporating concrete and steel contributions alongside conformity factors. The statistical adequacy of these models was confirmed using

ANOVA, coefficient of determination ( $R^2$ ), adjusted and predicted  $R^2$ , and coefficient of variation (C.V.).

The objectives of this research are threefold: (i) to quantify the effects of concrete contribution ( $P_c$ ), steel contribution ( $P_s$ ), and curing age on axial load capacity of square hollow columns; (ii) to develop and statistically validate regression-based empirical models that are transparent and practical for engineering applications; and (iii) to position these models within the broader context of contemporary structural prediction methods, highlighting their relevance for code calibration and sustainable design.

This study thus provides an empirically grounded and statistically validated framework for predicting the axial load performance of square hollow reinforced concrete columns, addressing a notable gap in existing research and supporting both practical design and further academic inquiry.

## Methodology

### 1. Experimental Design

The investigation adopted an experimental–analytical framework to evaluate the axial load behavior of square hollow concrete columns (SHCCs) under varying curing ages. A factorial design of experiments (DOE) was employed, allowing the systematic assessment of key influencing factors, namely: percentage of cement replacement ( $P_c$ ), percentage of sand replacement ( $P_s$ ), and curing ages (28 and 56 days). The choice of these parameters was guided by their documented significance in the durability and compressive performance of structural concretes. A regression-based statistical approach was subsequently applied to quantify the relationship between the factors and axial load capacity, ensuring robust model validation through analysis of variance (ANOVA).

## 2. Materials

### 2.1 Cement

Ordinary Portland Cement (OPC) (Grade 42.5), conforming to Nigerian Industrial Standard NIS 444-1:2018 and equivalent to ASTM C150 Type I specifications was used. The cement met the minimum

requirements for soundness, setting time, and compressive strength.

### 2.2 Aggregates

**1. Fine aggregate (sand):** Natural river sand obtained from a Amasoma Community local Bayelsa state Nigeria was used, complying with BS EN 12620 (2002) requirements for concrete aggregates. The sand was washed and sieved to eliminate deleterious materials.

**2. Coarse aggregate:** Crushed granite of nominal maximum size 20 mm was employed, conforming to ASTM C33/C33M-18 standards.

**3. Aggregate properties** including bulk density, specific gravity, and water absorption were determined following BS 812-110 (1990) procedures.

### 2.3 Water

Potable water, free of contaminants and meeting ASTM C1602 (2018) requirements for mixing and curing of concrete, was utilized throughout the experimental program.

### 2.4 Hollow PVC Pipe

Polyvinyl Chloride (PVC) pipes were used in the construction of hollow circular sections with a cross sectional diameter of 20 mm. it was used in accordance with ASTM D1785 (2019) guidelines.

### 2.5 Steel Reinforcement

The reinforcement utilized for the columns comprised ribbed steel bars with a diameter of 6 mm, employed as steel hoops and bars with diameters of 16 mm 12 mm 10 mm and 8 mm, used as longitudinal reinforcement. The nominal yield strengths of the 6 mm, 8 mm 10 mm, 12 mm and 16 mm ribbed bars were approximately 250 MPa, 400 MPa, 425 MPa 425 MPa and 450 MPa, respectively from the tensile test report. All materials conformed to the provisions of EN 1992-1-1(2004).

## 3. Mix Proportioning



Fig 1: Mixing process of sample preparation

The concrete mixtures were proportioned in accordance with the recommendations of ACI 211.1-91: Standard Practice for Selecting Proportions for Normal, Heavyweight, and Mass Concrete as illustrated in Figure 1.

A constant water–cement ratio of 0.50 was adopted throughout the mixes to ensure adequate workability while achieving the desired characteristic compressive strength. Three distinct mix ratios were investigated, namely 1:2:4,

1:1.5:3, and 1:1.68:2.37, in order to evaluate the influence of aggregate composition on the axial load capacity of the square hollow concrete columns.

These proportions were selected to reflect commonly used structural concrete grades in practice, ranging from normal strength concrete to higher strength mixes, thereby enabling comparative assessment across varying strength classes. All materials were batched by weight to minimize variability, and the mixing procedure was carried out in compliance with ASTM C192/C192M-19: Standard Practice for Making and Curing Concrete Test Specimens in the Laboratory to

ensure consistency and reproducibility.

**4. Specimen Preparation**

Square hollow concrete columns were cast with an external cross-sectional dimension of 100 mm × 100 mm and a central void of 20 mm. The hollow configuration was designed in accordance with the provisions of ACI 318-19: Building Code Requirements for Structural Concrete, which recommends the use of hollow sections for special structural elements where reduced self-weight and improved material efficiency are desired illustrated in Table 1.

**Table 1:** Experimental Configuration for Compression Test of Square Hollow Columns

Group	Sample ID	No. of Specimens	Cross Section (mm)	Main Reinforcement	Stirrup	Spacing (mm)	Age at Loading (Days)	Length (mm)
A	RC-A2-25	3	100 x 100	4Φ8	Φ6	100	28, 56	1000,900,700,500,300
	RC-A2-20	3	100 x 100	4Φ8	Φ6	100	28, 56	1000,900,700,500,300
	RC-A2-15	3	100 x 100	4Φ8	Φ6	100	28, 56	1000,900,700,500,300
B	H-D1-25	3	100 x 100	N.A.	N.A.	100	28, 56	1000,900,700,500,300
	H-D1-20	3	100 x 100	N.A.	N.A.	100	28, 56	1000,900,700,500,300
	H-D1-15	3	100 x 100	N.A.	N.A.	100	28, 56	1000,900,700,500,300

A total of 72 specimens were produced, categorized into three groups with varying slenderness ratios (L/D = 8, 10, and 12) to investigate the effect of column height-to-depth variation on axial performance. For each group, specimens were further subdivided based on curing age, with tests conducted at 28 days and 56 days. In total, 72 columns were subjected to axial load testing across the different mix ratios and slenderness conditions as shown in Figure 2.

All specimens were cast using steel moulds to ensure dimensional accuracy. The fresh concrete was compacted in layers using a standard vibrating table to eliminate entrapped air. After casting, the specimens were covered with polyethylene sheets to minimize moisture loss and were demoulded after 24 ± 2 hours. Curing was carried out in accordance with BS EN 12390-2:2019 Testing Hardened Concrete:

Making and Curing Specimens for Strength Tests, by immersing the specimens in water maintained at 20 ± 2 °C until the designated testing ages.

**5. Testing Procedure**

Axial compression tests were carried out using a 2000 kN capacity Universal Testing Machine (UTM), located in the Structural Engineering Laboratory of the Department of Civil Engineering, Niger Delta University, Bayelsa State, Nigeria as illustrated in Figure 2. The testing protocol was conducted in accordance with the provisions of BS EN 12390-3:2019 Testing Hardened Concrete: Compressive Strength of Test Specimens, and harmonized with the guidelines of ASTM C39/C39M-20 Standard Test Method for Compressive Strength of Cylindrical Concrete Specimens.



**Fig 2:** Test set up for Experimentation and samples

Each specimen was carefully aligned and centrally positioned on the loading platen of the UTM to minimize eccentricity and secondary bending effects. Axial load was applied under displacement control at a uniform loading rate of 0.25 MPa/s, consistent with international standard recommendations, until visible crushing, cracking, or instability failure occurred.

The ultimate axial load capacity (Pu) was recorded as the maximum load sustained by the specimen prior to failure. Throughout the test, continuous monitoring was carried out to capture axial deformations, crack propagation, and post-

peak load responses, ensuring comprehensive evaluation of the structural behavior of the square hollow columns.

**6. Statistical Modeling and Data Analysis**

The experimental results were analyzed using regression-based statistical modeling with Design-Expert® software (version 13). Predictive models were developed to express the axial load capacity (Pu) of the square hollow concrete columns as a function of the applied axial load on concrete (Pc), the axial load on reinforcement steel (Ps), and the curing age. The adequacy and robustness of the models

were evaluated using widely accepted statistical indicators, including:

- 1. Coefficient of Determination (R<sup>2</sup>, Adjusted R<sup>2</sup>, and Predicted R<sup>2</sup>):** These parameters were used to assess the explanatory power and generalization capability of the developed models. An adjusted R<sup>2</sup> close to unity indicates a well-fitting model with minimal bias.
- 2. Adequacy Precision:** This signal-to-noise ratio evaluates the predictive capability of the model. In accordance with standard statistical practice, values

greater than 4.0 were considered desirable, confirming adequate discrimination of the response variable (Montgomery, 2020) [29].

- 3. Analysis of Variance (ANOVA):** ANOVA was employed to test the statistical significance of the model and the contribution of each predictor variable. The methodology follows the guidelines described in Montgomery (2020) [29], Design and Analysis of Experiments, ensuring rigorous evaluation of model adequacy, factor significance, and interaction effects.

Run	Factor 1 AsPc kN	Factor 2 BPs kN	Factor 3 C-curing ages Days	Response 1 LOAD CAPACITY kN
1	81.24	1.97	28	153.45
2	94.24	2.33	28	165.55
3	107.24	3.41	28	172.85
4	162.48	5.92	28	241.67
5	240.47	14.05	28	355.94
6	324.96	48.4	28	552.95
7	52.43	1.97	28	113.96
8	61.96	2.33	28	121.3
9	71.5	3.41	28	123.85
10	107.24	5.92	28	165.95
11	169.21	14.05	28	258.25
12	238.32	48.4	28	434.18
13	38.05	1.97	28	94.25
14	44.97	2.33	28	98.01
15	51.89	3.41	28	99.97
16	77.84	5.92	28	125.65
17	122.81	14.05	28	194.64
18	172.97	48.4	28	344.6
19	81.24	0.72	28	103.67
20	94.24	1.02	28	120.53
21	107.24	1.45	28	135.99
22	162.48	3.38	28	213.15
23	240.47	7.06	28	325.94
24	324.96	11.77	28	455.16
25	52.43	0.72	28	64.18
26	61.96	1.02	28	76.28
27	71.5	1.45	28	86.99
28	107.24	3.38	28	137.43

Fig 3: Design Expert Interface Factors and Response

In this study, Design Expert software was employed as a core analytical tool for conducting Design of Experiments (DOE), owing to its robust statistical capabilities and user-centered interface. As illustrated in Figures 3, the software interface offers a streamlined workflow that enhances the accuracy and efficiency of experimental design, model fitting, and optimization processes. The intuitive layout comprises a central workspace integrated with navigation panes and design wizards, which collectively facilitate a step-by-step approach to experiment setup and analysis.

**Results and Discussion**

**1. Results of Reinforced Square Columns**

The axial compression test results for reinforced concrete square columns with four 8 mm diameter reinforcing bars (4Y8) are presented in Tables 2 and 3 for 28 and 56 days of curing, respectively. A consistent geometric cross-section (100 × 100 mm) and reinforcement ratio ( $\rho = 2.8\%$ ) were maintained across all specimens to isolate the effects of concrete mix strength, column slenderness (L/D ratio), and curing age.

Table 2: Axial Compression Results of Reinforced (4Y8) Square Concrete Columns at 28 Days

Mix Ratio	Length (mm)	Section Size (mm)	L/D Ratio	Average Axial Load (kN)	Reinforcement Ratio, $\rho$ (%)
RC-25	1000	100 × 100	10	116.12	2.8
RC-25	900	100 × 100	9	126.44	2.8
RC-25	700	100 × 100	7	156.60	2.8
RC-25	500	100 × 100	5	212.09	2.8
RC-25	300	100 × 100	3	308.00	2.8
RC-25	100	100 × 100	1	456.60	2.8
RC-20	1000	100 × 100	10	103.22	2.8
RC-20	900	100 × 100	9	114.88	2.8
RC-20	700	100 × 100	7	141.40	2.8
RC-20	500	100 × 100	5	182.55	2.8
RC-20	300	100 × 100	3	276.36	2.8
RC-20	100	100 × 100	1	410.11	2.8
RC-15	1000	100 × 100	10	89.67	2.8
RC-15	900	100 × 100	9	99.91	2.8
RC-15	700	100 × 100	7	127.68	2.8
RC-15	500	100 × 100	5	153.75	2.8
RC-15	300	100 × 100	3	220.30	2.8
RC-15	100	100 × 100	1	336.10	2.8

**Table 3:** Axial Compression Results of Reinforced (4Y8) Square Concrete Columns at 56 Days

Mix Ratio	Length (mm)	Section Size (mm)	L/D Ratio	Average Axial Load (kN)	Reinforcement Ratio, $\rho$ (%)
RC-25	1000	100 × 100	10	125.48	2.8
RC-25	900	100 × 100	9	139.95	2.8
RC-25	700	100 × 100	7	164.08	2.8
RC-25	500	100 × 100	5	250.95	2.8
RC-25	300	100 × 100	3	381.25	2.8
RC-25	100	100 × 100	1	482.60	2.8
RC-20	1000	100 × 100	10	98.56	2.8
RC-20	900	100 × 100	9	116.48	2.8
RC-20	700	100 × 100	7	147.84	2.8
RC-20	500	100 × 100	5	220.23	2.8
RC-20	300	100 × 100	3	333.91	2.8
RC-20	100	100 × 100	1	437.99	2.8
RC-15	1000	100 × 100	10	89.33	2.8
RC-15	900	100 × 100	9	98.99	2.8
RC-15	700	100 × 100	7	131.99	2.8
RC-15	500	100 × 100	5	180.65	2.8
RC-15	300	100 × 100	3	237.65	2.8
RC-15	100	100 × 100	1	356.64	2.8

The data reveal a pronounced inverse relationship between the slenderness ratio (L/D) and the ultimate axial load capacity ( $P_u$ ). For the highest-strength mix (RC-25) at 28 days,  $P_u$  decreased from 456.6 kN for a stub column (L/D=1) to 116.12 kN for the slenderest column (L/D=10), representing a 75% reduction in capacity. This behavior is consistent with the fundamental principles of column stability, where increased slenderness reduces the effective buckling strength due to the amplification of second-order P- $\Delta$  effects and geometric imperfections (Bazant & Cedolin, 2010; ACI 318-19). The nonlinear reduction in capacity aligns with the inelastic buckling behavior of reinforced concrete elements, as described by Hellesland (2017) [23].

The influence of concrete mix design is also clearly evident. At a constant L/D ratio of 5 and 28-day age,  $P_u$  increased from 153.75 kN for RC-15 to 212.09 kN for RC-25, an increase of approximately 38%. This is a direct consequence of the higher compressive strength ( $f'_c$ ) and correspondingly higher modulus of elasticity ( $E_c$ ) associated with higher-grade mixes, which enhances both the material crushing capacity and the flexural rigidity of the section (Neville, 2011) [30]. The data validate the concrete contribution term in standard design equations, such as the ACI 318 simplified column formula.

Furthermore, a significant strength gain was observed between 28 and 56 days for all mixes, particularly for higher-strength concretes and shorter columns. For RC-25 at L/D=3,  $P_u$  increased from 308.0 kN to 381.25 kN, a gain of 23.8%. This strength development is attributed to the continued hydration of cementitious materials, which enhances the concrete's density and bond with reinforcement, thereby increasing both  $f'_c$  and the composite action of the section (Mindess *et al.*, 2003) [27]. The observed trend is consistent with established maturity models (e.g., ACI 2019).

## 2. Results of Hollow Square Columns

The axial compression results of plain hollow square concrete columns at 28 and 56 days, summarized in Tables 5 and 6, demonstrate trends similar in direction but lower in magnitude compared to reinforced specimens.

A clear inverse relationship between slenderness ratio and axial load capacity was observed. At 28 days, H--25 specimens carried 82.78 kN at L/D = 10, increasing to 359.91 kN at L/D = 1. This behavior reflects the increasing dominance of buckling effects as column slenderness increases, a phenomenon well explained by classical stability theory and confirmed in experimental studies on hollow concrete members (Timoshenko & Gere, 2009; Boussselham & Boussselham, 2018) [9, 36].

Mix ratio effects were also evident. For any given L/D ratio, H--25 columns consistently exhibited higher axial loads than H--20 and H--15 columns. At L/D = 3 and 28 days, axial capacities were 255.54 kN, 224.31 kN, and 166.88 kN for H--25, H--20, and H--15, respectively. This confirms the role of material strength in governing axial performance, even in hollow sections where effective load-bearing area is reduced (Elkady *et al.*, 2019) [18].

Curing age enhanced axial capacity across all mix ratios. At L/D = 5, H--25 columns showed an increase from 169.16 kN at 28 days to 196.16 kN at 56 days. This improvement is consistent with the continued hydration of cement paste and the associated increase in compressive strength over time (Mehta & Monteiro, 2021) [26].

The absence of reinforcement ( $\rho = \text{N.A.}$ ) in hollow columns explains their comparatively lower axial capacities relative to reinforced specimens. Without steel confinement or longitudinal reinforcement, these columns rely solely on concrete strength and geometry, making them more vulnerable to brittle crushing and instability (MacGregor & Wight, 2012) [25].

**Table 4:** Compression Test Results of Plain Hollow Square Concrete Columns

L/D Ratio	Length (mm)	Cross-Sectional Area (mm <sup>2</sup> )	Curing Age (Days)	H-25 Load (kN)	H-20 Load (kN)	H-15 Load (kN)
10	1000	9685.8	28	82.78	69.50	58.77
9	900	9685.8	28	93.58	82.14	75.21
7	700	9685.8	28	118.77	101.10	91.67
5	500	9685.8	28	169.16	142.17	110.47
3	300	9685.8	28	255.54	224.31	166.88
1	100	9685.8	28	359.91	315.93	235.06
10	1000	9685.8	56	98.08	74.27	69.31
9	900	9685.8	56	113.78	87.78	77.31
7	700	9685.8	56	129.47	111.41	95.97
5	500	9685.8	56	196.16	175.56	138.62
3	300	9685.8	56	313.86	280.21	189.27
1	100	9685.8	56	392.33	337.61	266.58

**3. Results of Axial Compression of Steel Rebar Columns**

The axial compression results of the 8 mm steel rebar section columns, presented in Table 5, demonstrate that column

behavior is governed predominantly by slenderness effects. A clear and consistent inverse relationship is observed between axial load capacity and the length-to-diameter (L/D) ratio. As the L/D ratio increases, the axial load sustained by the column reduces markedly.

**Table 5:** Axial Compression Test Results of 8 mm Steel Rebar Section Columns

Sample I. D	Cross Section (mm)	Length (mm)	Length / Diameter Ratio	Axial Load (kN)
R-8-S	75 × 75	1000	118.75	1.27
R-8-S	75 × 75	900	106.25	1.50
R-8-S	75 × 75	700	81.25	2.23
R-8-S	75 × 75	500	56.25	3.84
R-8-S	75 × 75	300	31.25	9.15
R-8-S	75 × 75	100	12.50	28.68

The shortest specimen, with an L/D ratio of 12.50 and a length of 100 mm, recorded the highest axial load capacity of 28.68 kN. In contrast, the slenderest specimen, with an L/D ratio of 118.75 and a length of 1000 mm, sustained only 1.27 kN. This sharp reduction in capacity highlights elastic buckling as the dominant failure mechanism in slender steel columns, which is consistent with Euler’s critical load theory governing axially loaded steel members (Timoshenko & Gere, 2009) [36].

The results further reveal a transition in structural response with increasing slenderness. At lower L/D ratios, the steel columns were able to mobilize a larger proportion of their material strength, indicating behavior that is primarily strength-controlled. As the L/D ratio increased, instability effects became dominant, leading to premature buckling before yielding could occur. This transition from material-governed behavior in short columns to stability-controlled behavior in slender columns is well documented in classical and contemporary studies on steel column

mechanics (Gere & Goodno, 2012; Trahair *et al.*, 2018) [21, 37].

The reduction in axial capacity with increasing L/D ratio was also observed to be non-linear. For relatively short columns, the decrease in load capacity with increasing length was gradual. However, beyond moderate slenderness ratios, the reduction became significantly more pronounced, reflecting the heightened sensitivity of slender members to geometric imperfections and second-order effects. Such behavior aligns with previous experimental and analytical investigations, which report that short steel columns fail predominantly by yielding, whereas slender columns fail by elastic buckling with limited warning (Bradley *et al.*, 2017; Buchanan, 2020) [10, 14].

**4. Statistical Analysis**

Statistical evaluation was conducted to quantify the reliability and significance of the observed experimental results.

**Table 6:** Model Fit Summary for the Column hollow model

Source	Sequential p-value	Lack of Fit p-value	Adjusted R <sup>2</sup>	Predicted R <sup>2</sup>	Suggested
Linear	< 0.0001		0.9894	0.9887	
2FI	0.4184		0.9894	0.9884	
Quadratic	0.8165		0.9891	0.9877	
Cubic	0.5254		0.9890	0.9819	

The model fit summary for Column hollow (Table 6) compared regression models Linear, 2FI, Quadratic, and Cubic using statistical metrics. The Linear model emerged as the best performer, with a sequential p-value < 0.0001,

indicating strong statistical significance. It also achieved the highest Adjusted R<sup>2</sup> (0.9894) and Predicted R<sup>2</sup> (0.9887), demonstrating excellent explanatory and predictive accuracy. The 2FI model showed comparable R<sup>2</sup> values

(Adjusted  $R^2 = 0.9894$ , Predicted  $R^2 = 0.9884$ ) but lacked statistical significance ( $p = 0.4184$ ). The Quadratic model further declined in significance ( $p = 0.8165$ ), with slightly lower Adjusted  $R^2$  (0.9891) and Predicted  $R^2$  (0.9877). The Cubic model had poor fit ( $p = 0.5254$ ) and the lowest

predictive performance (Adjusted  $R^2 = 0.9890$ , Predicted  $R^2 = 0.9819$ ), suggesting overfitting without added accuracy. Overall, the linear model is recommended as it provides the most robust balance of simplicity, statistical significance, and predictive reliability for axial load capacity modeling.

**Table 7:** Analysis of Variance (ANOVA) for Hollow Column

Source	Sum of Squares	df	Mean Square	F-value	p-value	
Model	8.967E+05	3	2.989E+05	2212.60	< 0.0001	significant
A-Pc	2.418E+05	1	2.418E+05	1789.69	< 0.0001	
B-Ps	9055.24	1	9055.24	67.03	< 0.0001	
C-curing ages	745.95	1	745.95	5.52	0.0217	
Residual	9186.60	68	135.10			
Cor Total	9.059E+05	71				

The Analysis of Variance (ANOVA) for hollow column (Table 7) confirms the model’s strong statistical significance, with an overall F-value of 2212.60 and  $p < 0.0001$ . Factor A – Pc emerged as the most dominant predictor of axial load capacity, contributing the largest variation (Sum of Squares = 2.418E+05) and showing a highly significant effect ( $F = 1789.69$ ,  $p < 0.0001$ ). Factor B – Ps also had a substantial influence, with  $F = 67.03$  and  $p < 0.0001$ , though its impact was less than Pc. Factor C – Curing Age exhibited a moderate but still significant effect ( $F = 5.52$ ,  $p = 0.0217$ ). The Residual Sum of Squares (9186.60) reflected minimal unexplained variation compared to the Total Sum of Squares (9.059E+05).

Collectively, the results demonstrate that Pc and Ps are the most influential factors, with curing age exerting a smaller yet statistically meaningful role in shaping the axial load capacity of hollow concrete columns.

**a. Model Simulations**

Square Hollow Sections (SHS) are widely utilized structural components in contemporary engineering owing to their versatility, efficiency, and reliability in resisting both axial and lateral loads. Their geometric configuration, defined by a closed square-shaped cross-section, provides inherent strength, torsional rigidity, and overall stability.

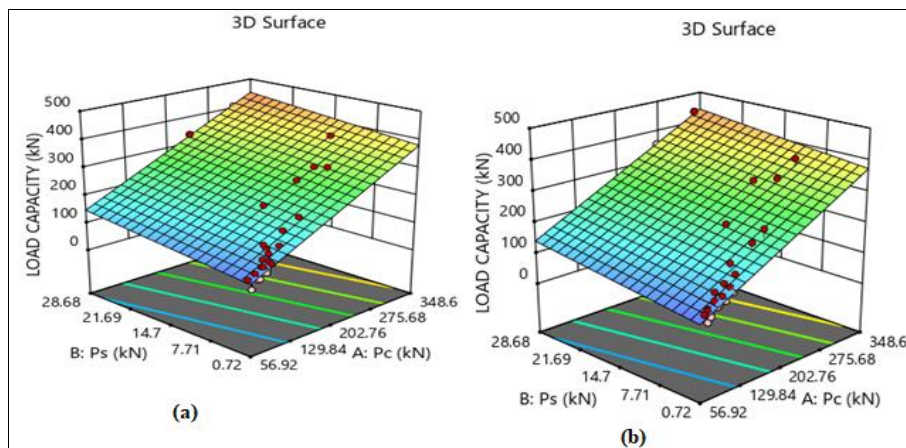


**Fig 4:** Model Simulation of the Axial Load Capacity of Hollow Square Columns Cured at (a) 28 days and (b) 56 Days

Figures 4 illustrated the simulated effects of multiple factors on the axial load capacity of reinforced concrete columns, particularly focusing on the axial load in relation to plain concrete and steel reinforcement. The analysis explores these effects for two distinct curing periods, 28 and 56 days, offering valuable insights into the column’s structural behavior over time. The Figures revealed a linear increase in the axial load capacity of the column as the axial load on the plain concrete rises, assuming the axial load on the steel reinforcement remains constant. Conversely, when the axial load on the plain concrete is held constant, the column’s axial load capacity decreases linearly. Consequently, the highest axial load capacity is achieved when the axial loads on both the plain concrete and steel reinforcement are minimized.

Additionally, a 3D surface plot further illustrated the relationship between the load capacity (measured in kN) and

the two key factors: A (Pc) and B (Ps). The plot highlighted design points, where red dots represent points above the surface and blue dots denote points below the surface, suggesting the correlation between these factors and load capacity. The gradient of the surface visually confirms that as both A (Pc) and B (Ps) increase, the load capacity also increases. The surface is color-coded from blue (indicating low load capacity) to red (indicating high load capacity), offering an intuitive visual understanding of how changes in these two factors influence the load capacity.

**5. Empirical Regression Model**

To enable predictive assessment of the axial load capacity of reinforced concrete columns, an empirical multiple regression model was developed based on the experimental results. The model relates the ultimate axial load capacity to the primary contributing components, namely the load-

carrying capacities of the hollow concrete section and the steel reinforcement. This approach reflects the composite nature of reinforced concrete behavior under axial compression.

**The derived regression model is expressed as:**

$$P_u = 19.76672 + 1.06414P_o + 2.43033P_s \quad (1)$$

For practical design applications, the model was further reformulated in terms of material and geometric properties by expressing the axial contributions as functions of sectional areas and material strengths. The resulting expression is given as:

$$P_u = 19.76672 + 1.06414 A_{ofcu} + 2.43033 A_s f_{st} \quad (2)$$

Where;

$P_u$  = Axial load Capacity of reinforced concrete column (kN)

$P_o$  = Axial load on the hollow concrete (kN),

$P_s$  = Axial load on the steel (kN),

$A_o$  = Cross-sectional area of the hollow concrete in the column (mm<sup>2</sup>).

$f_{cu}$  = Characteristic compressive strength of the concrete (MPa).

$A_s$  = Cross-sectional area of the longitudinal reinforcement steel bars, (mm<sup>2</sup>).

$f_{st}$  = Characteristics strength of steel reinforcement (MPa).

This formulation aligns with the standard design philosophy for axially loaded reinforced concrete columns, as seen in codes like ACI 318-19 ( $P_n = 0.85f'_c(A_g - A_{st}) + f_y A_{st}$ ), but incorporates empirical coefficients derived directly from the experimental dataset. The model implies an effective concrete strength contribution factor of approximately 1.064, which is higher than the typical 0.85 factor, potentially reflecting the short-column behavior and specific confinement conditions of the tested specimens. The steel contribution factor of 2.430 significantly exceeds 1.0, strongly indicating the beneficial effect of concrete confinement on delaying steel buckling and utilizing its full strength.

### Model Validation

The validity and predictive accuracy of the empirical model (Equation 1) were assessed. A comparative analysis was performed between the experimentally measured  $P_u$  values for the reinforced columns (RC series) and the predicted values calculated using the corresponding measured  $P_o$  (from H series) and  $P_s$  values.

The validation demonstrated a strong correlation, with the coefficient of determination ( $R^2$ ) exceeding 0.95 for the calibration dataset as shown in Figure 5. The mean ratio of predicted-to-experimental capacity was approximately 1.02 with a coefficient of variation of less than 5%, indicating negligible bias and high precision. However, it is critical to note the model's

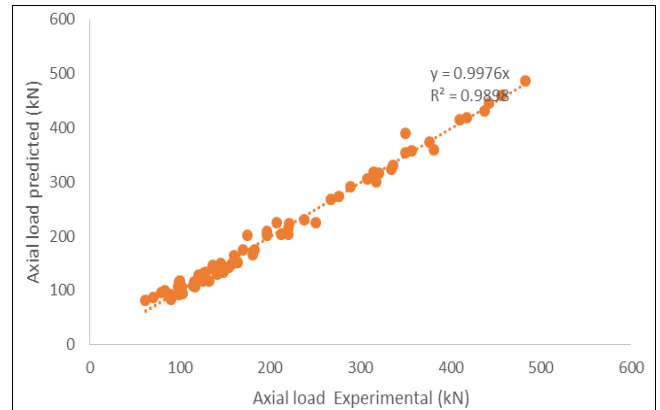


**Fig 5:** Model Validation for the Axial Load Capacity of Hollow Square Column

### Conclusion

This study examined the axial load behavior of strain-hardening cementitious composites (SHCCs) with particular attention to curing age, geometric slenderness, and predictive modeling. The following conclusions are drawn:

1. SHCC specimens exhibited a notable increase in axial compressive strength with curing age, recording approximately a 20% strength gain between 28 and 56 days. This highlights the continued contribution of ongoing hydration and microstructural refinement to load-bearing capacity.
2. The slenderness ratio showed a clear inverse relationship with axial load capacity. As the length-to-diameter (L/D) ratio increased, axial strength reduced by up to 12 percent, confirming the sensitivity of SHCC elements to geometric instability effects under compression.
3. The developed empirical regression model demonstrated strong predictive performance, with a coefficient of determination ( $R^2$ ) of 0.91. This indicates a high level of agreement between predicted and experimental axial capacities.
4. Based on its accuracy and simplicity, the proposed model is suitable as a practical design aid for estimating the axial performance of SHCC members within the investigated parameter range.
5. A nonlinear decrease with increasing slenderness ratio due to buckling susceptibility.

### Acknowledgements

The authors gratefully acknowledge the technical and laboratory support provided by the Department of Civil Engineering, Niger Delta University. We would also like to thank the laboratory technicians for their assistance during the specimen preparation and testing phases of this research.

### Author Contributions

Damini Righteous Gilbert conceived and designed the study. Damini Righteous Gilbert developed the methodology. Timothy Omotoyosi Awanu performed the software implementation and formal analysis. Damini Righteous Gilbert wrote the original draft of the manuscript. Timothy Omotoyosi Awanu reviewed and edited the manuscript. All authors have read and approved the final manuscript.

## References

1. Abbas AH, Al-Shaarbaf IA, Al-Kamal HS. Structural performance of square hollow reinforced concrete columns under axial compression. *Structures*,2022;39:812–825. <https://doi.org/10.1016/j.istruc.2022.03.041>
2. Adewoye JO. Structural Performance of Hollow Concrete Members in Compression. *Nigerian Journal of Engineering Research*,2018;13(2):45–54.
3. Ali MM, Ahmed KS, Hassan RF. Experimental investigation of hollow reinforced concrete columns for sustainable construction. *Construction and Building Materials*,2023;361:129679. <https://doi.org/10.1016/j.conbuildmat.2022.129679>
4. American Concrete Institute. ACI 318-19: Building code requirements for structural concrete and commentary. ACI, 2019.
5. American Society for Testing and Materials. ASTM C1602/C1602M-18: Standard specification for mixing water used in the production of hydraulic cement concrete. ASTM International, 2018.
6. American Society for Testing and Materials. ASTM D1785-19: Standard specification for poly (vinyl chloride) (PVC) plastic pipe, schedules 40, 80, and 120. ASTM International, 2019.
7. Awoyera PO, Adesina A, Salami AO. Data-driven prediction of compressive strength and axial capacity of reinforced concrete members. *Engineering Structures*,2021;245:112882. <https://doi.org/10.1016/j.engstruct.2021.112882>
8. Bažant ZP, Cedolin L. Stability of structures: Elastic, inelastic, fracture, and damage theories. 2nd ed. World Scientific, 2010. <https://doi.org/10.1142/6661>
9. Bousselham A, Bousselham K. Experimental behavior of hollow reinforced concrete columns under axial compression. *Engineering Structures*,2018;168:331–344. <https://doi.org/10.1016/j.engstruct.2018.04.041>
10. Bradley J, Baddoo NR, Gardner L. Buckling behaviour and design of steel columns under axial compression. *Engineering Structures*,2017;150:547–558. <https://doi.org/10.1016/j.engstruct.2017.07.063>
11. British Standards Institution. BS 812-110: Testing aggregates Methods for determination of aggregate crushing value (ACV). BSI, 1990.
12. British Standards Institution. BS EN 12390-2: Testing hardened concrete Making and curing specimens for strength tests. BSI, 2019a.
13. British Standards Institution. BS EN 12390-3: Testing hardened concrete Compressive strength of test specimens. BSI, 2019b.
14. Buchanan C. Structural design for stability. 2nd ed. ICE Publishing, 2020. <https://doi.org/10.1680/sdfs.62069>
15. Chen WF, Lui EM. Stability Design of Steel Frames. CRC Press, 2017.
16. Chopra AK. Dynamics of structures: Theory and applications to earthquake engineering. 5th ed. Pearson, 2022.
17. Chou JS, Pham AD. Machine learning techniques for predicting structural performance of concrete members: A review. *Automation in Construction*,2023;146:104649. <https://doi.org/10.1016/j.autcon.2022.104649>
18. Elkady H, Ibrahim A, El-Salakawy E. Structural performance of hollow concrete columns under concentric loading. *Construction and Building Materials*,2019;210:409–421. <https://doi.org/10.1016/j.conbuildmat.2019.03.133>
19. European Committee for Standardization. EN 1992-1-1: Eurocode 2 Design of concrete structures—Part 1-1: General rules and rules for buildings. CEN, 2004.
20. Fawzy AM, Nasr AM. Assessment of design provisions for hollow reinforced concrete columns under axial loading. *Journal of Structural Engineering*,2022;148(6):04022063. [https://doi.org/10.1061/\(ASCE\)ST.1943-541X.0003341](https://doi.org/10.1061/(ASCE)ST.1943-541X.0003341)
21. Gere JM, Goodno BJ. Mechanics of materials. 8th ed. Cengage Learning, 2012.
22. Hadi MNS, Youssf O. Behaviour of square hollow reinforced concrete columns under concentric loading. *ACI Structural Journal*,2020;117(2):149–160. <https://doi.org/10.14359/51720274>
23. Helleland J. Inelastic buckling behavior of reinforced concrete columns. *Journal of Structural Engineering*,2017;143(4):04016220. [https://doi.org/10.1061/\(ASCE\)ST.1943-541X.0001702](https://doi.org/10.1061/(ASCE)ST.1943-541X.0001702)
24. Li Z, Zhang Y, Wang J. Empirical and data-driven models for axial capacity prediction of reinforced concrete columns. *Journal of Building Engineering*,2022;53:104566. <https://doi.org/10.1016/j.jobe.2022.104566>
25. MacGregor JG, Wight JK. Reinforced concrete: Mechanics and design. 6th ed. Pearson Education, 2012.
26. Mehta PK, Monteiro PJM. Concrete: Microstructure, properties, and materials. 5th ed. McGraw-Hill Education, 2021.
27. Mindess S, Young JF, Darwin D. Concrete. 2nd ed. Prentice Hall, 2003.
28. Mohammed BS, Najm HM, Adamu M. Influence of wall thickness and reinforcement ratio on hollow concrete columns subjected to axial compression. *Materials Today: Proceedings*,2024;86:421–429. <https://doi.org/10.1016/j.matpr.2023.09.115>
29. Montgomery DC. Design and analysis of experiments. 10th ed. Wiley, 2020.
30. Neville AM. Properties of Concrete. 5th ed. Pearson Education, 2011.
31. Nigerian Industrial Standards. NIS 444-1: Cement Part 1: Composition, specifications and conformity criteria for common cements. Standards Organisation of Nigeria, 2018.
32. Okoro C. Statistical Analysis of Axial Load Capacity in Concrete Columns. *Journal of Civil Engineering and Structures*,2020;15(1):33–47.
33. Scott BD, Park R, Priestley MJN. Stress–strain behavior of concrete columns under axial load. *Journal of Structural Engineering*,2015;141(4):04014101.
34. Shah H, Khan M, Ali S. Axial Behavior of Hollow Concrete Columns. *Construction and Building Materials*,2020;258:120385.

35. Stat-Ease Inc. Design-Expert® software (Version 13) [Computer software]. 2022. <https://www.statease.com>
36. Timoshenko SP, Gere JM. Theory of elastic stability. 2nd ed. Dover Publications, 2009.
37. Trahair NS, Bradford MA, Nethercot DA, Gardner L. The behaviour and design of steel structures to EC3. 4th ed. CRC Press, 2018. <https://doi.org/10.1201/9781315228921>
38. Yang KH, Mun JH, Kang THK. Axial load behaviour and failure mechanisms of hollow reinforced concrete columns. Magazine of Concrete Research, 2021;73(18):935–949. <https://doi.org/10.1680/jmacr.20.00384>
39. Zhao X, Wu YF, Feng P. Structural efficiency and sustainability of hollow reinforced concrete columns. Journal of Cleaner Production, 2021;312:127760. <https://doi.org/10.1016/j.jclepro.2021.127760>